



# Strong coupling in a microcavity containing $\beta$ -carotene

RICHARD T. GRANT,<sup>1,4</sup> RAHUL JAYAPRAKASH,<sup>1,4,\*</sup> DAVID M COLES,<sup>1</sup>  
ANDREW MUSSER,<sup>1</sup> SIMONE DE LIBERATO,<sup>2</sup> IFOR D.W. SAMUEL,<sup>3</sup>  
GRAHAM A. TURNBULL,<sup>3</sup> JENNY CLARK,<sup>1</sup> AND DAVID G. LIDZEY<sup>1</sup>

<sup>1</sup>Department of Physics and Astronomy, The University of Sheffield, Hicks Building, Hounsfield Road, Sheffield S3 7RH, UK

<sup>2</sup>Department of Physics and Astronomy, University of Southampton, Southampton, SO17 1BJ, UK

<sup>3</sup>Organics Semiconductor Centre, SUPA, School of Physics & Astronomy, University of St Andrews, St Andrews, Fife KY 16 9SS, UK

<sup>4</sup>Richard T. Grant & Rahul Jayaprakash have made equal contribution to the work

\*[r.jayaprakash@sheffield.ac.uk](mailto:r.jayaprakash@sheffield.ac.uk)

**Abstract:** We have fabricated an open-cavity microcavity structure containing a thin film of the biologically-derived molecule  $\beta$ -carotene. We show that the  $\beta$ -carotene absorption can be described in terms of a series of Lorentzian functions that approximate the 0-0, 0-1, 0-2, 0-3 and 0-4 electronic and vibronic transitions. On placing this molecular material into a microcavity, we obtain anti-crossing between the cavity mode and the 0-1 vibronic transition, however other electronic and vibronic transitions remain in the intermediate or weak-coupling regime due to their lower oscillator strength and broader linewidth. We discuss the consequences of strong-coupling for the possible modification of photosynthetic processes, or a re-ordering of allowed and optically-forbidden states.

© 2018 Optical Society of America under the terms of the [OSA Open Access Publishing Agreement](#)

**OCIS codes:** (130.0250) Optoelectronics; (160.4670) Optical materials; (160.4760) Optical properties; (160.4890) Organic materials; (230.1150) All-optical devices; (230.4040) Mirrors; (240.5420) Polaritons; (300.1030) Absorption; (300.3700) Linewidth; (350.3950) Micro-optics.

## References and links

1. M. S. Skolnick, T. A. Fisher, and D. M. Whittaker, "Strong coupling phenomena in quantum microcavity structures," *Semicond. Sci. Technol.* **13**(7), 645–669 (1998).
2. K. J. Vahala, "Optical microcavities," *Nature* **424**(6950), 839–846 (2003).
3. D. Bajoni, E. Semenova, A. Lemaître, S. Bouchoule, E. Wertz, P. Senellart, and J. Bloch, "Polariton light-emitting diode in a GaAs-based microcavity," *Phys. Rev. B* **77**(11), 113303 (2008).
4. M. Richard, J. Kasprzak, R. André, L. S. Dang, and R. Romestain, "Angle resolved spectroscopy of polariton stimulation under non-resonant excitation in CdTe II–VI microcavity," *J. Phys. Condens. Matter* **16**(35), S3683–S3688 (2004).
5. L. K. van Vugt, S. Rühle, P. Ravindran, H. C. Gerritsen, L. Kuipers, and D. Vanmaekelbergh, "Exciton Polaritons Confined in a ZnO Nanowire Cavity," *Phys. Rev. Lett.* **97**(14), 147401 (2006).
6. G. Christmann, R. Butté, E. Feltin, A. Mouti, P. A. Stadelmann, A. Castiglia, J.-F. Carlin, and N. Grandjean, "Large vacuum Rabi splitting in a multiple quantum well GaN-based microcavity in the strong-coupling regime," *Phys. Rev. B* **77**(8), 85310 (2008).
7. D. G. Lidzey, D. D. C. Bradley, M. S. Skolnick, T. Virgili, S. Walker, and D. M. Whittaker, "Strong exciton–photon coupling in an organic semiconductor microcavity," *Nature* **395**(6697), 53–55 (1998).
8. J. R. Tischler, M. S. Bradley, V. Bulović, J. H. Song, and A. Nurmikko, "Strong Coupling in a Microcavity LED," *Phys. Rev. Lett.* **95**(3), 036401 (2005).
9. D. Ballarín, M. De Giorgi, S. Gambino, G. Lerario, M. Mazzeo, A. Genco, G. Accorsi, C. Giansante, S. Colella, S. D'Agostino, P. Cazzato, D. Sanvitto, and G. Gigli, "Polariton-Induced Enhanced Emission from an Organic Dye under the Strong Coupling Regime," *Adv. Opt. Mater.* **2**(11), 1076–1081 (2014).
10. S. Kéna-Cohen, S. A. Maier, and D. D. C. Bradley, "Ultrastrongly Coupled Exciton-Polaritons in Metal-Clad Organic Semiconductor Microcavities," *Adv. Opt. Mater.* **1**(11), 827–833 (2013).
11. J. D. Plumhof, T. Stöfeler, L. Mai, U. Scherf, and R. F. Mahrt, "Room-temperature Bose-Einstein condensation of cavity exciton-polaritons in a polymer," *Nat. Mater.* **13**(3), 247–252 (2014).
12. K. S. Daskalakis, S. A. Maier, R. Murray, and S. Kéna-Cohen, "Nonlinear interactions in an organic polariton condensate," *Nat. Mater.* **13**(3), 271–278 (2014).
13. R. T. Grant, P. Michetti, A. J. Musser, P. Gregoire, T. Virgili, E. Vella, M. Cavazzini, K. Georgiou, F. Galeotti,

- C. Clark, J. Clark, C. Silva, and D. G. Lidzey, "Efficient Radiative Pumping of Polaritons in a Strongly Coupled Microcavity by a Fluorescent Molecular Dye," *Adv. Opt. Mater.* **4**(10), 1615–1623 (2016).
14. E. Orgiu, J. George, J. A. Hutchison, E. Devaux, J. F. Dayen, B. Doudin, F. Stellacci, C. Genet, J. Schachenmayer, C. Genes, G. Pupillo, P. Samorì, and T. W. Ebbesen, "Conductivity in organic semiconductors hybridized with the vacuum field," *Nat. Mater.* **14**(11), 1123–1129 (2015).
  15. A. Thomas, J. George, A. Shalabney, M. Dryzhakov, S. J. Varma, J. Moran, T. Chervy, X. Zhong, E. Devaux, C. Genet, J. A. Hutchison, and T. W. Ebbesen, "Ground-State Chemical Reactivity under Vibrational Coupling to the Vacuum Electromagnetic Field," *Angew. Chem. Int. Ed. Engl.* **55**(38), 11462–11466 (2016).
  16. F. Herrera and F. C. Spano, "Cavity-Controlled Chemistry in Molecular Ensembles," *Phys. Rev. Lett.* **116**(23), 238301 (2016).
  17. T. W. Ebbesen, "Hybrid Light-Matter States in a Molecular and Material Science Perspective," *Acc. Chem. Res.* **49**(11), 2403–2412 (2016).
  18. D. M. Coles, Y. Yang, Y. Wang, R. T. Grant, R. A. Taylor, S. K. Saikin, A. Aspuru-Guzik, D. G. Lidzey, J. K.-H. Tang, and J. M. Smith, "Strong coupling between chlorosomes of photosynthetic bacteria and a confined optical cavity mode," *Nat. Commun.* **5**, 5561 (2014).
  19. D. M. Coles, N. Somaschi, P. Michetti, C. Clark, P. G. Lagoudakis, P. G. Savvidis, and D. G. Lidzey, "Polariton-mediated energy transfer between organic dyes in a strongly coupled optical microcavity," *Nat. Mater.* **13**(7), 712–719 (2014).
  20. X. Zhong, T. Chervy, S. Wang, J. George, A. Thomas, J. A. Hutchison, E. Devaux, C. Genet, and T. W. Ebbesen, "Non-Radiative Energy Transfer Mediated by Hybrid Light-Matter States," *Angew. Chem. Int. Ed. Engl.* **55**(21), 6202–6206 (2016).
  21. G. D. Scholes, G. R. Fleming, A. Olaya-Castro, and R. van Grondelle, "Lessons from nature about solar light harvesting," *Nat. Chem.* **3**(10), 763–774 (2011).
  22. K. Stamatakis, M. Tsimilli-Michael, and G. C. Papageorgiou, "On the question of the light-harvesting role of  $\beta$ -carotene in photosystem II and photosystem I core complexes," *Plant Physiol. Biochem.* **81**, 121–127 (2014).
  23. A. Telfer, "What is  $\beta$ -carotene doing in the photosystem II reaction centre?" *Philos. Trans. R. Soc. B Biol. Sci.* **357**, 1431 (2002).
  24. T. Polívka and V. Sundström, "Ultrafast Dynamics of Carotenoid Excited States-From Solution to Natural and Artificial Systems," *Chem. Rev.* **104**(4), 2021–2072 (2004).
  25. R. Houdré, "Early stages of continuous wave experiments on cavity-polaritons," *Phys. Status Solidi* **242**(11), 2167–2196 (2005).
  26. V. Savona, L. C. Andreani, P. Schwendimann, and A. Quattropani, "Quantum well excitons in semiconductor microcavities: Unified treatment of weak and strong coupling regimes," *Solid State Commun.* **93**(9), 733–739 (1995).
  27. S. A. Furman and A. V. Tikhonravov, "Spectral Characteristics of Multi-Layer Coatings: Theory," in *Basics of Optics of Multilayer Systems* (Atlantica Séguier Frontières, 1992).
  28. R. Jayaprakash, "Transfer matrix model for open cavity data analysis," figshare (2017) [retrieved 11 October 2017], <https://figshare.com/s/cc4d67677f614c733e3e>.
  29. R. Jayaprakash, "Coupled oscillator model for open cavity data analysis," figshare (2017) [retrieved 11 October 2017], <https://figshare.com/s/7726f55f7dd7f73f8cee>.

## 1. Introduction

Cavity-polaritons are hybrid light-matter states that can be formed when a semiconductor is placed inside an optical microcavity [1,2]. The resonant, reversible exchange of energy between the semiconductor exciton and confined cavity-photon yields a splitting of these states into lower and upper polaritons, separated by the Rabi splitting energy ( $\hbar\Omega$ ). This phenomenon has been widely investigated in both inorganic [3–6] and organic semiconductors [7–10], the latter of which have the advantage of strongly bound excitons that are stable at room temperature. Recent advances have seen the development of organic exciton-polariton condensates and room-temperature polariton lasing [11,12], and an ever-expanding field of molecules capable of undergoing strong exciton-photon coupling [13].

The formation of cavity-polariton states in molecular semiconductors can have profound effects, even before the onset of condensation. It has been argued that the creation of delocalised polariton states in a molecular film can be used to modulate charge-transport properties [14], change activation barriers [15,16] and potentially allow control over chemical reactivity landscapes [17]. In multicomponent, multi-exciton systems, this alteration of energy levels may also perturb electronic energy transfer-pathways in complex molecular assemblies; for example by strong coupling chlorosomes in bacterial light harvesting complexes [18]. In the limit in which multiple excitonic states can each separately enter the strong-coupling regime, hybrid polariton states form that are a mixture of the cavity photon

and the different excitonic components. Such ‘hybrid’ states can be used to mediate rapid and efficient energy transfer over extremely long distances through the highly delocalised photon component, and have been proposed as model systems in which energy transfer in light-harvesting systems may be explored [19,20].

The concept of modified energy relaxation has been clearly demonstrated in the case of distinct J-aggregates [19,20], but is of greater interest in light-harvesting systems such as the archetypal photosynthetic complexes [21]. It has already been shown that the primary component of these complexes – chlorophylls – is capable of strong coupling [18]. In this paper, we investigate the potential for polariton formation using another chromophore that is essential in biological light-harvesting; namely  $\beta$ -carotene [see chemical structure in Fig. 1(a)].  $\beta$ -carotene is abundant in plants, fungi and photosynthetic bacteria, and absorbs strongly in the blue to blue-green spectral region. This and related carotenoids are widely considered to serve as efficient antennas to funnel light energy to chlorophyll during photosynthesis [22,23]. The ability to create polaritonic states using  $\beta$ -carotene can potentially be seen as a step towards being able to modify photosynthetic process in various organisms using an entirely photonic approach.

We note that strong coupling in carotenoids opens up a further intriguing possibility that arises from the unique electronic structure of these molecules, as shown in Fig. 1(b). Carotenoids, as polyenes, have the unusual characteristic that the lowest-energy singlet electronic state ( $2A_g = S_1$ ) shares the same spatial symmetry ( $A_g$ ) as the ground state and is thus dark to one-photon transitions [24]. The first allowed electronic transition thus occurs into the higher-energy  $1B_u = S_2$  state. On excitation, the excited state relaxes into the dark  $S_1$  at a rate that greatly exceeds photoluminescence ( $\tau \sim 200$  fs), making the molecules almost completely non-emissive [24]. In the strong-coupling regime, the formation of polariton states thus has the potential to alter this energy-level ordering by bringing the emissive  $S_2$ -coupled polariton states below the energy of  $S_1$ , as shown in Fig. 1(b), thereby turning a dark molecule bright. To explore whether such effects can be observed in practice, we have explored strong coupling in pure films of  $\beta$ -carotene placed inside an optical microcavity. Via measurement of cavity transmission spectra and detailed transfer-matrix modelling, we demonstrate the presence of polariton states formed by optical coupling to the 0-1 vibronic transition. The Rabi-splitting observed here however is relatively small ( $\sim 140$  meV), and thus at present a direct re-ordering of bright and dark-states is not currently possible using this material. Nevertheless, we expect the ability to strongly couple  $\beta$ -carotene also to exist in other photosynthetic systems, which may allow a modification of the local energy landscape and thus perturb energy relaxation processes.

## 2. Methods

The microcavities explored here were based on a so-called ‘open-cavity’ architecture. Here, a layer of  $\beta$ -carotene was deposited by spin-coating onto a fused silica substrate that had been coated with a 20 nm thick silver film. The films were spin-cast from a 40mg/mL THF solution at 500rpm, and had a thickness between 950 and 1100 nm. A typical absorption spectrum of a 200nm  $\beta$ -carotene film prepared from the same solution at a spin speed of 2000rpm, is shown in Fig. 1(c). A second mirror also formed from a 20 nm thick film of silver on a  $100\mu\text{m} \times 100\mu\text{m}$  fused silica plinth (created using a diamond saw) was then positioned close to the surface of the  $\beta$ -carotene film using a series of manual position controllers and piezo-stages. This created the microcavity-structure having a Q-factor of  $\sim 100$  as shown schematically in Fig. 1(d). Control films of  $\beta$ -carotene were also prepared on fused silica substrates, with their

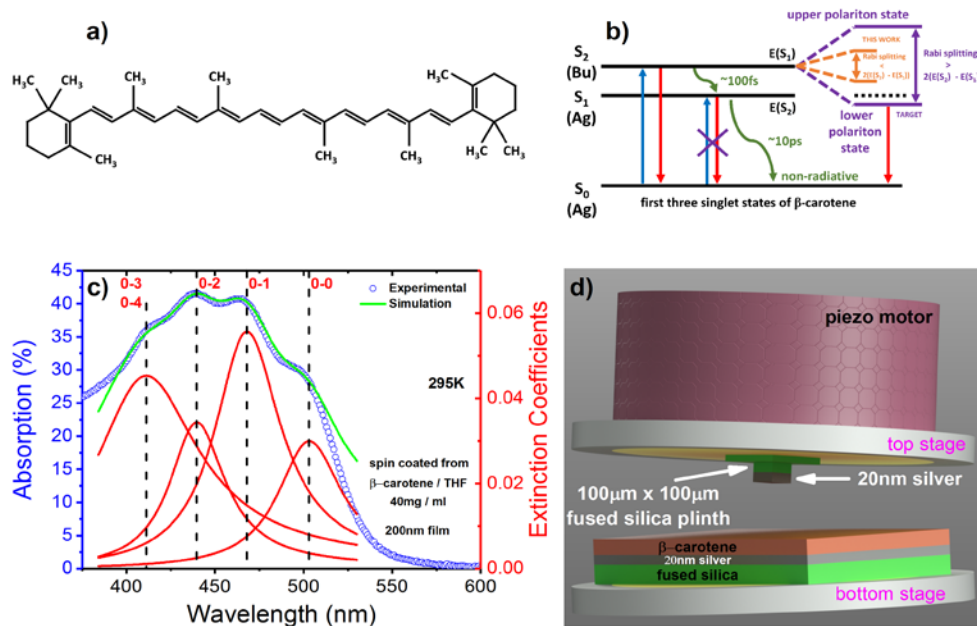


Fig. 1. Part (a) shows the chemical structure of  $\beta$ -carotene. Part (b) shows a simplified energy-level diagram of the electronic states of  $\beta$ -carotene and indicates its allowed and forbidden electronic transitions. We also indicate the possible effects of optical strong-coupling to the  $S_2$  transition. Part (c) shows the absorption spectrum of a thin-film of  $\beta$ -carotene as deposited onto a quartz substrate. Here, we make a fit to the absorption spectrum using four Lorentzian functions, and identify the location of the 0-0, 0-1, 0-2 and 0-3 transitions. Finally, part (d) shows a schematic of the open-cavity system.

optical absorption characterised using a Horiba Jobin Yvon Fluoromax-4 spectrofluorometer equipped with F3031 transmission accessory. Note that during the course of the research it was found that  $\beta$ -carotene is highly susceptible to photo-oxidation. For this reason, all films were prepared in a nitrogen-filled glovebox. However the open-cavity system was operated under ambient conditions, and thus it is highly likely that the  $\beta$ -carotene film underwent some photo-degradation both before and during measurement. Indeed, as we show below, the oscillator strength of the films studied is relatively low.

To characterise the microcavities, their optical transmission was measured as a function of mirror separation (cavity length). This permitted the relative separation (and thus interaction strength) between the cavity mode and the  $\beta$ -carotene excitonic resonances to be controlled in a dynamic fashion. To do this, light from a tungsten lamp was imaged onto the cavity via a long focal length (100mm) lens. Light transmitted through the cavity was then collected using a 50X Mitutoyo Plan Apo SL infinity corrected objective and then delivered to an imaging spectrograph (Andor Shamrock SR193i) having a resolution of 2.5 nm at 500 nm.

### 3. Results and Discussion

Figure 1(c) plots the absorption spectrum of a control  $\beta$ -carotene film. It can be seen that the absorption is characterised by a broad band that extends over the wavelength-range 400 – 550 nm. We have fitted the measured absorption spectrum using a transfer matrix reflectivity model in which we include four separate Lorentzian functions having different linewidths and oscillator strength. Figure 1(c) shows the result of the fit – it can be seen that we accurately reproduce the absorption peaks at 503, 468, 440 and 410 nm. However our fit fails to accurately reproduce the measured absorption at longer wavelengths, and suggests that the use of Lorentzian functions to fully describe the electronic structure of  $\beta$ -carotene is an over

simplification. Nevertheless we believe this approach adequately describes the electronic structure of  $\beta$ -carotene around its peak absorption wavelengths. It can be seen that there are absorption maxima peaks at 503, 468 and 440 nm that most likely correspond to transitions from the  $S_0$  ground state to the 0-0, 0-1 and 0-2 vibronic states of the  $S_2$  excited-state manifold. Such transitions have full-width half maximum linewidths (FWHM) of 42, 48 and 37 nm respectively. The peak at 410 nm is likely to be an un-resolved combination of the 0-3 and 0-4 transitions and thus has a significantly broader linewidth of 75 nm.

Figure 2(a) plots the optical transmission of an open-cavity as the cavity length is varied from 991 to 1255 nm. Here, the cavity length ( $L$ ) corresponds to the distance between the top mirror and the bottom mirror and is given by the sum of the thickness of the active layer ( $L_{active}$ ) and thickness of the air-gap ( $L_{air}$ ) between the active layer and the top mirror. To determine cavity length, it is first necessary to calculate the mode numbers ( $q$ ) of the various optical modes using

$$q = \frac{\lambda_{q-1}}{\lambda_{q-1} - \lambda_q}. \quad (1)$$

Here,  $\lambda_q$  and  $\lambda_{q-1}$  correspond to the wavelength of the  $q^{th}$  and  $(q-1)^{th}$  mode respectively. Using this analysis, we are able to identify modes  $q = 7, 8, 9$  and 10 within the transmission spectrum shown in Fig. 2(a). The mode number ( $q$ ) in turn can then be related to the cavity length ( $L$ ) using

$$L = \frac{q \cdot \lambda_q}{2n(\lambda_q)} \quad (2)$$

where  $n(\lambda_q)$  corresponds to an average refractive index of the active layer and air at  $\lambda_q$ . Note that during the experiments, it was found to be possible to push the top mirror into the  $\beta$ -carotene film as it had a soft, gel-like consistency as a result of residual casting-solvent that remained trapped in the film. This permitted cavity lengths to be explored that were less than  $L_{active}$ .

In Fig. 2(a), we indicate the wavelength of the electronic and vibronic transitions of  $\beta$ -carotene as determined from the absorption spectrum shown in Fig. 1(c). It can be seen that at least three optical modes (7, 8 and 9) interact (cross or anti-cross) with the various vibronic transitions. Indeed, mode  $q = 7$  clearly interacts with the 0-1 vibronic transitions, although the anti-crossing behaviour is initially hard to resolve. The interaction of mode  $q = 7$  with the  $\beta$ -carotene vibronic transitions can be more clearly seen by plotting selected transmission spectra corresponding to cavity lengths between 991 and 1168 nm as shown in Fig. 2(b). Here, at a cavity length of 995 nm, modes 7 and 8 are visible at 513 and 404 nm respectively. As the cavity-length is reduced, these modes undergo a blue-shift, with mode  $q = 7$  visibly 'crossing' the 0-0 transition at 503 nm. This crossing behaviour indicates that the 0-0 transition of  $\beta$ -carotene remains in the weak-coupling regime within the cavity.

As the cavity length is progressively reduced, mode  $q = 7$  then undergoes anti-crossing (strong-coupling) with the 0-1 transition located at 440 nm. The interaction with the 0-2 transition at 468 nm is less clear, and we suspect that the interaction with this mode is either in the intermediate / weak-coupling regime [25,26]. The strong interaction with the 0-1 mode



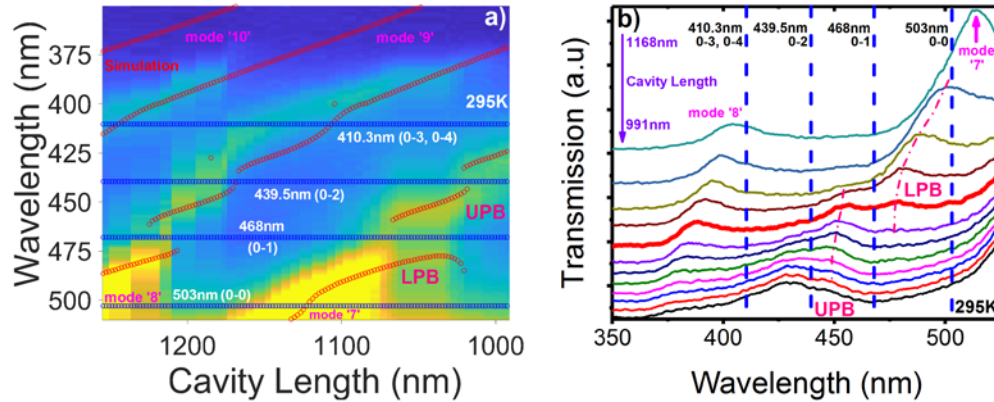


Fig. 2. Part (a) shows a 3D map of the optical transmission through the microcavity as a function of cavity length and wavelength. Here, high transmission is indicated using yellow, with low transmission using blue. On this Fig. we indicate the wavelength of the different absorptive transitions of  $\beta$ -carotene using horizontal lines, and indicate the mode number ( $q$ ) of the various optical modes. Here mode 7 undergoes anti-crossing around the 0-1 transition. We are therefore able to identify the upper and lower polariton branches (UPB and LPB). The red circles correspond to simulation using TM model. Part (b) shows measured optical transmission spectra at different cavity path-lengths. Again, we mark the wavelengths of the  $\beta$ -carotene transitions, together with the UPB and LPB. The dot dashed pink lines indicating the polariton branches are a guide to the eye.

results in the formation of two polariton branches that we label as the lower and upper polariton branches (LPB, UPB). Note that the dotted lines included in Fig. 2(b) indicating the polariton branch energy are a guide to the eye rather than a fit to the data. From Fig. 2(b), it is evident that mode  $q = 7$  does not cross the unresolved 0-3 / 0-4 transition at 410 nm transition, indicating that these states also remain in the weak-coupled regime.

To account for the dispersion of the observed polariton branches and estimate the Rabi splitting associated with the different transitions, a Transfer Matrix (TM) model [27] depicted in Code 1 [28] was used to simulate the open cavity transmission spectra as a function of cavity length. As input to the model we use four Lorentzian functions to describe the various electronic / vibronic transitions whose peak position and linewidth were extracted from the absorption spectrum shown in Fig. 1(c). We also use a background refractive index of 1.45 and then fit the TM simulation to the measured dispersion by adjusting the overall oscillator strength of the various transitions (whilst keeping their relative strength fixed as defined by the measured absorption spectrum).

Figure 2(a) plots the results of the TM simulation of the cavity modes using red circles. It can be seen that this provides a qualitatively good fit to the experimental data, and describes the dispersion of modes  $q = 7, 8, 9$  and 10. We compare the dispersion of the various optical modes with the experimentally measured peak positions in Fig. 3 for cavity lengths 1000 to 1140 nm. This confirms that mode  $q = 8$  undergoes crossing behaviour (weakly-coupled) with the 0-3 / 0-4 vibronic transition. Our model and data indicates that mode 7 undergoes energetic-crossing with the 0-0 mode indicating that it is weakly coupled. We do however evidence anti-crossing between mode 7 and the 0-1 transition and determine a Rabi splitting (energetic separation) between LPB and UPB of  $\sim 140$  meV. Note that the Rabi-splitting energy is larger than the linewidth of the LPB and UPB around resonance (which have a FWHM of  $\sim 128$  meV) indicating that this transition is strongly-coupled. We detect some energetic interaction with the 0-2 mode, however the estimated level of the Rabi-splitting here is  $\sim 116$  meV; a value that is

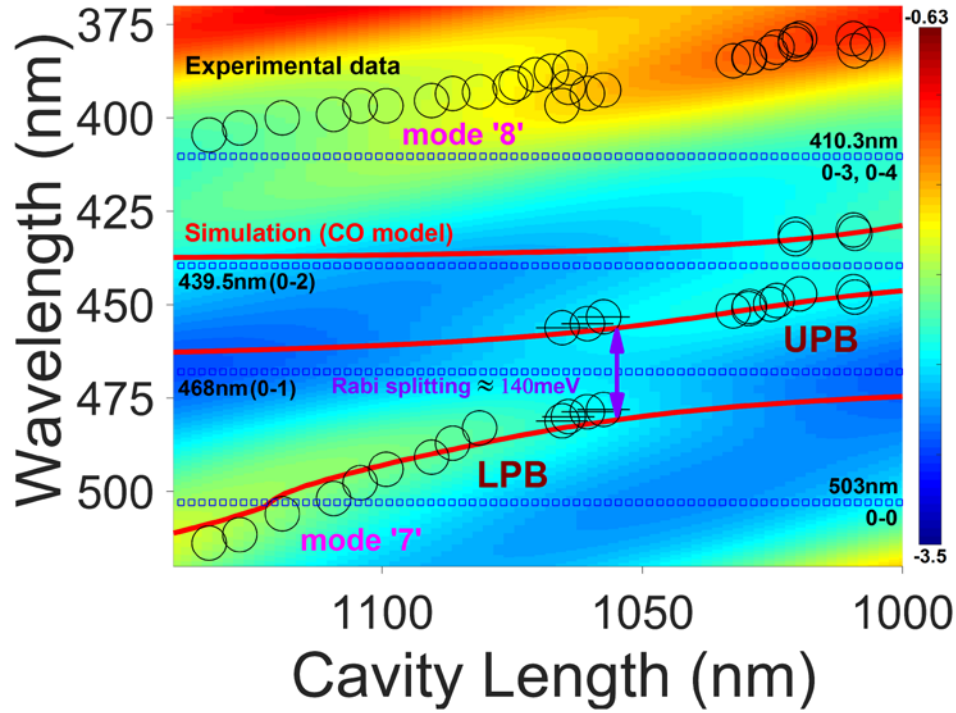


Fig. 3. 3D TM simulation of transmission as a function of cavity length and wavelength. Here black circles are experimental data points determined from the transmission spectra and the red lines correspond to simulations derived from the Coupled Oscillator (CO) model. The wavelengths of the  $\beta$ -carotene transitions, together with the UPB and LPB are marked.

somewhat smaller than the linewidth of the individual polariton-like branches which have a linewidth of around 135 meV. For this reason, we label such a transition as being in the intermediate / weak coupling regime. It should also be noted that mode  $q = 7$  does not cross the 0-3, 0-4 transition. The fact that only the 0-1 mode is observed to undergo strong coupling is partly explained by the fact that the peak extinction coefficient of the 0-1 vibronic mode is 30% larger than that of the 0-0 and 0-2 modes [see Fig. 1(c)] and thus the Rabi-splitting energy for interaction with the 0-1 mode is expected to be larger [1].

However to gain further insight into the strong coupling between mode  $q = 7$  and 0-1 transition, a  $5 \times 5$  Coupled Oscillator (CO) model [26] detailed in [Code 2](#) [29] was used to simulate the open cavity transmission spectra as a function of cavity length. The position of the individual transitions and their respective linewidths (half-width at half maximum [HWHM]) derived from the fit to the absorption spectrum [see Fig. 1(c)] were used as the input to the model. The model accurately simulates the experimental data as shown in Fig. 3 using the following coupling constants ( $g$ ) and HWHM linewidths ( $\gamma$ ) corresponding to the different transitions:

$$\begin{aligned}
 g_{0-0} &= 0.037eV & \gamma_{0-0} &= 0.108eV \\
 g_{0-1} &= 0.091eV & \gamma_{0-1} &= 0.128eV \\
 g_{0-2} &= 0.070eV & \gamma_{0-2} &= 0.122eV \\
 g_{0-3,0-4} &= 0.105eV & \gamma_{0-3,0-4} &= 0.256eV
 \end{aligned}$$

Here a Rabi splitting value of the 0-1 transition with mode  $q = 7$  was again determined as 140 meV. We note strong coupling to an isolated state usually needs to satisfy the following condition:

$$g_{0-1}^2 > \frac{1}{2}(\gamma_{0-1}^2 + \gamma_{cav}^2). \quad (3)$$

If we use values of  $g_{0-1} = 0.091\text{eV}$ ,  $\gamma_{0-1} = 0.128\text{eV}$  and  $\gamma_{cav} = 0.0125\text{eV}$  (derived from the measured HWHM cavity-mode linewidth and corresponding to a Q-factor of  $\sim 100$ ) we find

$\sqrt{\frac{1}{2}(\gamma_{0-1}^2 + \gamma_{cav}^2)} = 0.0909$ ; a result consistent with the 0-1 transition reaching the strong-coupling regime.

Our results demonstrate therefore that a biomolecule found in many different types of photosynthetic organisms can be placed into a microcavity and undergo strong-coupling. This finding follows on from previously reported work [18], in which the chlorosomes of a light-harvesting bacteria were shown to undergo strong-coupling. Here, we strong-couple to one of a number of relatively broad transitions in the molecule  $\beta$ -carotene. This suggests that in a suitably designed microcavity, it may be possible to strong-couple to  $\beta$ -carotene when it is contained within a photosynthetic complex; a result that may permit energy relaxation and transfer processes to be modified through control of the local electromagnetic environment. We note that the Rabi-splittings achieved here are too small to permit a re-ordering of states as illustrated in Fig. 1(b). Indeed, the energy separation between the S1 and S2 states is of the order of 800 meV, suggesting that a significant increase in interaction energies are needed to realise this scheme. As discussed above, we believe that the extreme photosensitivity of  $\beta$ -carotene films to photooxidation may well account for reduced oscillator strengths and thus reduced Rabi-splitting energies. Future experiments are planned to mitigate such unwanted oxidation reactions.

In summary therefore, we have fabricated open-cavity structures containing the molecular dye  $\beta$ -carotene, and have found that it is possible to strong-couple the 0-1 vibronic mode of the molecule to an optical cavity mode, with a Rabi-splitting of 140 meV evidenced. We speculate that photo-oxidation of  $\beta$ -carotene thin films may reduce its effective oscillator strength and prevents other electronic and vibronic transitions from also undergoing strong-coupling.

## Funding

UK EPSRC (EP/M025330/1).

## Acknowledgments

We thank the UK EPSRC for funding a PhD scholarship for R.T.G. S.D.L. gratefully acknowledges the Royal Society Research fellowship. We would also like to thank Jason Smith and Lucas Flatten for providing the plinths, which have been extensively used in the open cavity measurements. The raw experimental data can be accessed through the online research data repository of The University of Sheffield – ORDA: <https://figshare.com/s/cc4d67677f614c733e3e>, <https://figshare.com/s/7726f55f7dd7f73f8cee>.